ELSEVIER

Polymer 41 (2000) 8375–8385

polymer

www.elsevier.nl/locate/polymer

Role of inherent matrix toughness on fracture of glass bead filled epoxies

J. Lee[1,a], A.F. Yee[b,*]

[a]*Macromolecular Science and Engineering Center, The University of Michigan, Ann Arbor, MI 48109, USA*
[b]*Department of Materials Science and Engineering, The University of Michigan, Ann Arbor, MI 48109, USA*

Received 2 December 1999; received in revised form 24 February 2000; accepted 24 February 2000

Abstract

Some polymers can be toughened by rigid inorganic fillers. In this study, the effect of inherent matrix toughness on the fracture of filled thermosets is systematically investigated using glass beads and epoxies. The toughening effect of glass beads, i.e. the relative increase of toughness due to the incorporation of glass beads, follows an increase in the molecular weight of epoxides. Inherent matrix toughness is found to increase with the increase of the epoxide molecular weight. Microscopy studies reveal that the sizes of debonding and micro-shear banding zones are increased as the fracture toughness of composites increases. Matrix shear yielding is identified as one of the major energy absorbing mechanisms for unmodified and modified epoxies.

Keywords: Inorganic particle toughening; Fracture toughness; Epoxy

1. Introduction

Although the use of inorganic particles as fillers in many polymers is widespread, our knowledge about the fracture behavior of inorganic particle filled composites has developed very slowly. Many questions remain regarding fracture behavior, major toughening sources and the extent of their contribution to the toughness of inorganic particle filled polymers. The effect of inherent matrix ductility on the fracture toughness of filled thermosets is the subject of the current investigation.

Cross-link density, such as those measured by the molecular weight between cross-links, can determine the fracture toughness of thermoset polymers [1,2]. When thermoset polymers are toughened by the addition of inorganic particles, the inherent matrix toughness can affect the resulting increase in fracture toughness. If we compare several experimental results in literature [3–13], it can be found that toughening has been achieved for both brittle [3–10] and ductile [11] epoxy matrices. Furthermore, a generalization can be easily found in the literature [12], which is that the toughening effect of inorganic particle inclusion in thermosets decreases as inherent matrix toughness increases.

An experiment using two types of urethane methacrylate polymers, one of which contained a soft-block and the other did not, revealed that fracture toughness increases due to inorganic particle incorporation into both polymers [12]. The more pronounced increase is found in the latter system. It was reported in this experiment that the polymer containing the soft-block was more ductile [12]. It may not be appropriate to generalize from the result of this research because the two polymers used in this experiment have very different chemical structures, which lead to differences in fracture behavior.

In one of the early studies on glass bead filled thermoplastics [13], it was reported that the ductile matrix, polyphenylene oxide, can be toughened by the incorporation of glass beads, but the toughness increase in this system is smaller than those found in more brittle matrix systems, such as toughened polystyrene or poly(styrene-*co*-acrylonitrile). This report also cannot unambiguously explain the effect of inherent matrix toughness, again, because the basis for comparison is not controlled. All polymers used in this experiment have different fracture behavior, so it is difficult to compare their increase in toughness due to inorganic particle inclusion. By the same token, even if this conclusion is true for toughened thermoplastic polymers, it may not be generally true for thermoset polymers. Therefore, a systematic study is needed to address the relationship between the inherent toughness of the thermoset matrix and

* Corresponding author. Fax: + 1-734-763-4788.
E-mail addresses: jong@cems.umn.edu (J. Lee), afyee@engin.umich.edu (A.F. Yee).
[1] Current address: Department of Chemical Engineering and Materials Science, University of Minnesota, Minneapolis, MN 55455, USA.

0032-3861/00/$ - see front matter
PII: S0032-3861(00)00186-5

Table 1
Physical properties of unmodified epoxies

Epoxy resins (Designation)	DER 332®/DDS (332)	DER 661®/DDS (661)	DER 664®/DDS (664)	DER 667®/DDS (667)
Density (g/cm^2)	1.238	1.204	1.194	1.188
K_{IC} (MPa m$^{1/2}$)	0.78 (±0.12)	0.86 (±0.097)	1.11 (±0.053)	1.28 (±0.092)
Modulus (GPa)	2.95 (±0.09)	2.8 (±0.15)	2.83 (±0.14)	2.85 (±0.16)
Epoxide M_W (g/mol)	334–352	950–1150	1750–1950	3200–4000
T_g (K)	502	397	384	372
M_c from T_g (g/mol)	283	1182	1950	4875
M_c from rubbery shear modulus (g/mol)	439	1074	1446	5396
Plastic zone size calculated, $2r_p$ (μm)	–	10	20	29

the fracture toughness of the particulate composites it may form.

The major toughening mechanism for inorganic particle filled polymers is widely believed to be the crack front bowing mechanism [14–19]. According to this mechanism, particles in a brittle matrix can resist crack propagation by making the crack front bow out between particles. The amount of line energy in the bowed crack front reflects the toughness increase due to the existence of particles. This mechanism explains the common generalization on the effect of inherent matrix toughness [12,20], that is the toughening effect of inorganic particle incorporation into polymers decreases as inherent matrix toughness increases. The increase of inherent matrix toughness allows more glass beads to debond from the matrix, so the crack bowing ability of particles (impenetrability) decreases. However, the crack bowing theory neither identifies the origin of the impenetrability [21] nor shows the relationship between the impenetrability and the extent of debonding. Furthermore, studies on the filled epoxies does not significantly depend on the extent of debonding. Therefore, the crack bowing theory could not properly explain the effect of inherent matrix toughness.

In the current study, a series of glass bead filled epoxies is used to investigate the effect of inherent matrix toughness on fracture behavior. The inherent matrix toughness is systematically varied by changing the molecular weight of epoxides. Increasing the molecular weight of epoxides decreases the cross-link density of epoxies, resulting in the increase of inherent matrix toughness. Since the same curing agent is used in all composites, by changing the cross-link density of the matrix, the chemical nature of matrices is changed in a systematic manner. An unexpected discovery on the effect of inherent matrix toughness will be reported and successfully explained by our study on micromechanical deformations instead of the crack front bowing mechanism.

2. Experimental

2.1. Materials

Glass beads (G) used in this experiment are Spheriglass® A-glass beads (soda-lime) with no surface treatment purchased from the Potters Industry Co. The mean diameters of glass beads measured by the liquid-phase sedimentation method using a Horiba CAPA-700 particle size analyzer and optical microscopy were 24.4 and 27.9 μm, respectively [43–46]. Four different kinds of epoxides, DER 332®, 661®, 664®, 667®, are diglycidyl ether of bisphenol A (DGEBA) resins produced by the Dow Chemical Co. Their molecular weights (epoxide MW) can be found in Table 1. All other reagents including 4,4′-diaminodiphenylsulphone (DDS, 98%) and solvents were obtained from Aldrich Chemical Co. and used without further purification.

Glass beads were cleaned with distilled water as follows: 290 g of glass beads were dispersed in 1 L of distilled water under mechanical stirring at room temperature for 6 h and the water was filtered out. This cleaning step was repeated three times. The cleaned glass beads were then dried under vacuum at 70°C for 12 h and their aggregates were screened out using a 75 μm sieve (mesh size = 200).

Table 2
Curing procedure for epoxy resins

Resin	Degassing/mixing with glass beads	Degassing/mixing with DDS	Curing	Post-curing
332	80°C, 1.5 h	120°C, 3 h	120°C, 13 h	250°C, 2 h
661	160°C, 1.5 h	160°C, 40 min	160°C, 15 h 20 min	200°C, 2 h
664	160°C, 1.5 h	160°C, 30 min	160°C, 15 h 30 min	200°C, 2 h
667	160°C, 1.5 h	160°C, 20 min	160°C, 15 h 40 min	200°C, 2 h

2.2. Preparation of composites

The mixing and curing schedules can be found in Table 2. Before curing, all epoxides were first degassed under vacuum for about one and a half hours at the mixing temperature (the first step in Table 2). To prevent glass beads from settling to the bottom of the mold during curing, the time for degassing/mixing with DDS was varied according to the types of epoxides. Total curing time (the second and the third steps in Table 2) was 16 h regardless of the type of epoxides. After mixing, the degassed mixture was poured into a preheated metal mold, vertically mounted in a convection oven and cured. The oven was then switched off and the cured resin was allowed to cool slowly to room temperature in the oven.

2.3. Characterization

To determine the cross-link density (Table 1), the rubbery shear moduli of unmodified (neat) epoxies were measured at 50°C above T_g by using a Bohlin Rheometer CS-50. Samples of 1 mm thickness were tested in a parallel plate geometry (PP20®). In a frequency sweep from 0.01 to 10 Hz, the average modulus value of the plateau region was taken to be the rubbery shear modulus. In fact, the frequency dependence of shear modulus at this temperature was found to be very small. The number average molecular weight between cross-links (M_c) (Table 1) was calculated using the theory of rubber elasticity [25].

$$M_c = q\rho RT/G_c \tag{1}$$

where q is the front factor (0.725 in this work [1]), T temperature (K), ρ the density at temperature T, G_c the equilibrium modulus in the rubbery region at temperature T, and R the universal gas constant. Although this equation has been widely used to determine cross-link density, it cannot give precise M_c values, because the networks of epoxies used here could not be ideally Gaussian and have an unknown amount of elastically inactive chains.

The glass transition temperature (T_g) of epoxies was measured using a differential scanning calorimeter (DSC), a Perkin–Elmer DSC-7. The heating rate was 10°C/min and sample weights were 6–9 mg. Since no significant differences were found between the first and the second scans, the temperature of the deflection point in the first scan was chosen as T_g. The T_g of an unmodified epoxy matrix was found to be 124°C.

For the assessment of fracture toughness, the critical stress intensity factor (K_{IC}) of epoxies was measured by fracturing single-edge-notched (SEN) type specimens in the three-point bend (3PB) geometry (span = 50.8 mm). Specimens were cut and polished into 6.35 (thickness, B) × 12.7 (width, W) mm size which meets the plane strain condition requirement [20]. A sharp notch was introduced by tapping a hammer on a razor blade inserted into the sample. The razor blade had been previously cooled in liquid nitrogen before it was used to make a notch. The tip of the crack was created by the wedging action of the razor. A screw-driven Instron machine (Instron 4502) was used at a crosshead speed of 2.54 mm/min. The K_{IC} values were determined using the relationship [26,27]

$$K_{IC} = Y\frac{3PS\sqrt{a}}{2BW^2}$$

$$Y = 1.93 - 3.07(a/W) + 14.53(a/W)^2 - 25.11(a/W)^3 + 25.80(a/W)^4 \tag{2}$$

where Y is a shape factor, P the load at failure, S the length of the span, and a the crack length. Twelve to eighteen specimens of an epoxy composite were tested. Critical strain energy release rates (G_{IC}) (plane stress conditions) were calculated from the stress intensity values using the following relationship [27]:

$$G_{IC} = \frac{K_{IC}^2}{E} \tag{3}$$

Scanning electron microscopy investigation was performed on the fracture surface of SEN-3PB specimens coated with a thin layer of gold–palladium using a Hitachi S-800 SEM. The accelerating voltage was either 5 or 3 kV.

The double-edge-notched four-point bend (DEN-4PB) technique [28] was used to create sub-critically loaded cracks. First, specimens having two almost identical cracks on the same edge were prepared and fractured in four-point bend geometry. Since the two cracks cannot be identical, one of the cracks will grow sub-critically and stop before failure, while the other breaks. After the sub-critically loaded cracks were prepared, thin sections taken from this test sample's mid-plane [28] were observed using an optical microscope (OM), Nikon Microphot II.

The petrographic thin-sectioning technique [28–31] was used to prepare thin-sections for OM investigation on subsurface damage and sub-critically loaded crack tips. The specimens of DEN-4PB and SEN-3PB tests were polished using rough to fine silicon carbide (SiC) grinding discs (grit size 80, 250, 400, 600, 1000) and alumina suspensions (5, 1, 0.3, 0.05 μm), until the thickness of around 40 μm was reached. At least two thin-sections were prepared and examined for each glass bead filled epoxy resin. To identify possible surface artifacts, all thin-sections were first examined using a reflected light OM.

In addition to the fracture toughness measurement, uniaxial tensile tests (ASTM D 638) were also performed using the same screw-driven Instron machine (crosshead speed = 2.54 mm/min). Specimens having a gauge section of 15 × 5 × 7 mm were prepared, and the surface of specimens was polished using SiC grinding discs (grit size 80, 240, 400, 600). More than five specimens were tested to obtain the modulus of a composite.

Table 3
Mechanical properties of modified epoxies

Epoxy resins	10 vol% G/332	10 vol% G/661	10 vol% G/664	10 vol% G/667
K_{IC} (MPa $m^{1/2}$)	1.09 (±0.058)	1.50 (±0.054)	1.99 (±0.054)	2.54 (±0.091)
K_{IC} (G modified)/K_{IC} (unmodified)	1.40	1.74	1.76	1.98
Modulus (GPa)	3.42 (±0.15)	3.66 (±0.24)	3.61 (±0.16)	3.33 (±0.20)
Debonding zone site (μm)	–	54 (±13)	116 (±34)	143 (±21)
G_{IC} (G modified)/G_{IC} (unmodified)	1.68	2.33	2.52	3.37

3. Results and discussion

3.1. Mechanical properties of composites

The molecular weight of epoxides is varied to systematically change inherent matrix toughness and study its effect on inorganic particle toughening. Therefore, the correlation between the molecular weight of epoxides and inherent matrix toughness needs explanation. Since the major energy absorption mechanism in the fracture of unmodified epoxy resins is thought to be local plastic deformation at the crack tip [20], the important factor in determining inherent matrix toughness is how much intrinsic plasticity the macromolecular network is capable of. If the density of cross-links increases, the 'deformability' of the network will decrease. Therefore, inherent matrix toughness is expected to decrease with the increase of cross-link density which can be controlled by changing the molecular weight of epoxides [32]. However, in reality, the effect of the molecular weight change is not that simple. In addition to the change in cross-link density, the chemistry of the network can be changed as well. As the molecular weight of epoxides increases, the contents of sulfone and amine groups in resins decrease, while the content of ether groups increases. Unfortunately, the effect of this chemical nature on cross-link density and inherent matrix toughness is difficult to assess. Regardless of the molecular basis, the inherent matrix toughness is successfully increased by increasing the molecular weight of epoxides, as can be seen in Table 1.

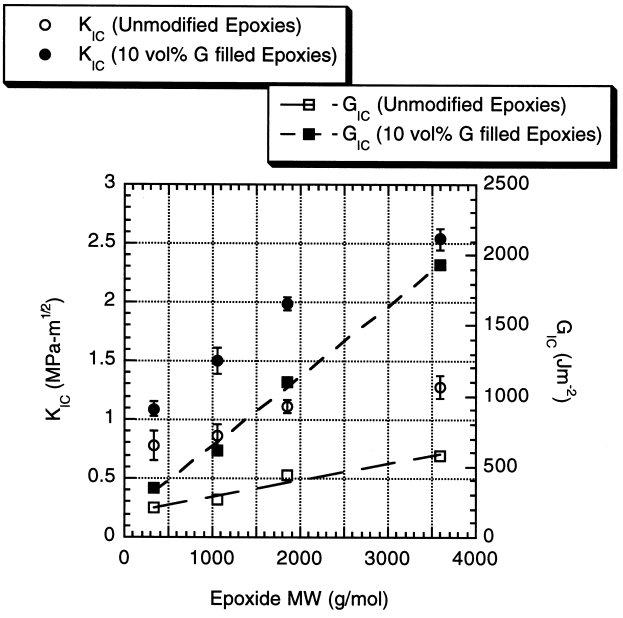

Fig. 1. Effect of epoxide molecular weight (MW) on the critical stress intensity factor (K_{IC}) and the critical strain energy release rate (G_{IC}) of glass bead filled epoxies.

To determine the cross-link density, the density of physical cross-links (entanglements) as well as chemical cross-links must be considered. Glad and Kramer [33] reported that the entanglement molecular weight (M_e) of bisphenol-A epoxy resins is about 4200–5050 g/mol. Although this value is not precisely the M_e of our epoxies, approximate estimation on the density of physical cross-links can be made using this value, because there is a very close similarity between the chemical structures of their epoxies and those used in this work. The M_e value is generally larger than the measured average molecular weights between cross-links (M_c) in Table 1. Therefore, the density of chemical cross-links is likely to be significantly larger than that of physical cross-links. Consequently, only the effect of chemical cross-links will be considered in the current approach.

M_c of epoxy resins can be calculated from their T_g using an empirical equation [34]

$$T_g - T_g^0 = \frac{3.9 \times 10^4}{M_c} \tag{4}$$

where T_g^0 is the glass transition temperature of the corresponding linear polymer. For DGEBA/DDS epoxy resins, T_g^0 was reported to be 364 K [35]. The calculated values from this equation are presented in Table 1. They show the same trend as the M_c values obtained using Eq. (1). The M_c values in Table 1 also show reasonable agreement in their trends with the results of Pearson and Yee [1]. They studied the effect of cross-link density on the toughening effect of *rubber* particles incorporation using the same series of epoxy matrices as used in here. In Tables 1 and 3, the basic physical properties of unmodified epoxies and composites are presented.

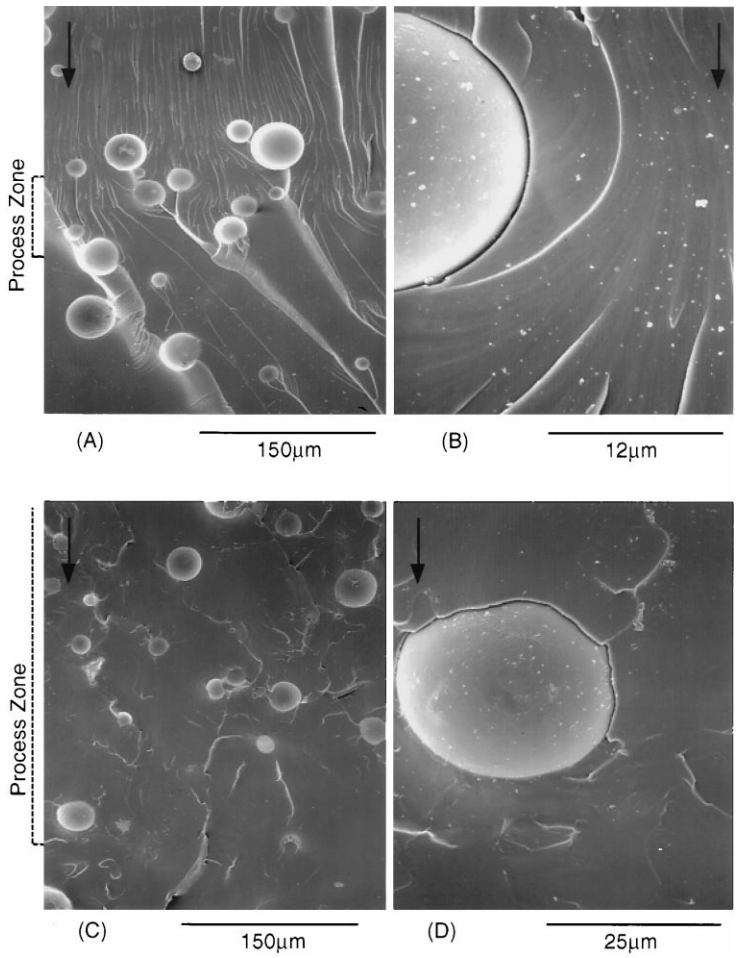

Fig. 2. SEM micrographs of the fracture surface of SEN-3PB specimens (process zone): (A) and (B) 10 vol% G/332; (C) and (D) 10 vol% G/667. The arrows indicate the direction of crack propagation.

Fig. 1 shows the fracture toughness with respect to the molecular weight of epoxides. The K_{IC} and G_{IC} data show the same dependence of fracture toughness on the molecular weight of epoxides: as the molecular weight increases, the fracture toughness of both unmodified and glass bead filled epoxies increases as well. The rate of increase of fracture toughness per unit increase of epoxide molecular weight is larger in glass bead filled epoxies that in unmodified epoxies. In other words, the relative increase of toughness due to the incorporation of glass beads, K_{IC}(modified)/K_{IC}(unmodified), becomes larger with the increase of the molecular weight of epoxides. Table 3 shows two relative increases, K_{IC}(modified)/K_{IC}(unmodified) and G_{IC}(modified)/G_{IC}(unmodified), which have the same trend. From this result, it can be concluded that the toughening effect of glass bead incorporation is larger in tougher matrices. This trend is contrary to what is commonly expected [12,20]; viz. the toughening effect due to inorganic particle incorporation decreases as the inherent matrix toughness increases. Our results do not support this common generalization. In fact, the generalization is not based on conclusive evidences, but by comparing experimental results obtained from different filled composites having different fracture behaviors [12,13], as mentioned above.

It could be argued that the increase in the toughening effect with increasing epoxide molecular weight found in Fig. 1 results from changes in the interfacial strength between glass beads and matrix, instead of changes in the inherent matrix toughness. As mentioned above, as the molecular weight of epoxides increases, the contents of sulfone and amine groups decrease, and ether groups increase. As a result, the interfacial strength can decrease, because the sulfone and amine functional groups might strengthen the chemical and physical interactions between glass beads and epoxy matrix more than ether groups. This possible series of events could make the study on the effect of inherent matrix toughness difficult and complicated. Fortunately, it has been reported [3,4,22–24] that the fracture toughness of glass bead filled epoxies does not significantly depend on the increase or decrease of interfacial strength altered by changing the content of any specific functional group on glass bead surface. Consequently, the increase of toughening effect found in Fig. 1 can be better explained in terms of changes in the inherent matrix toughness.

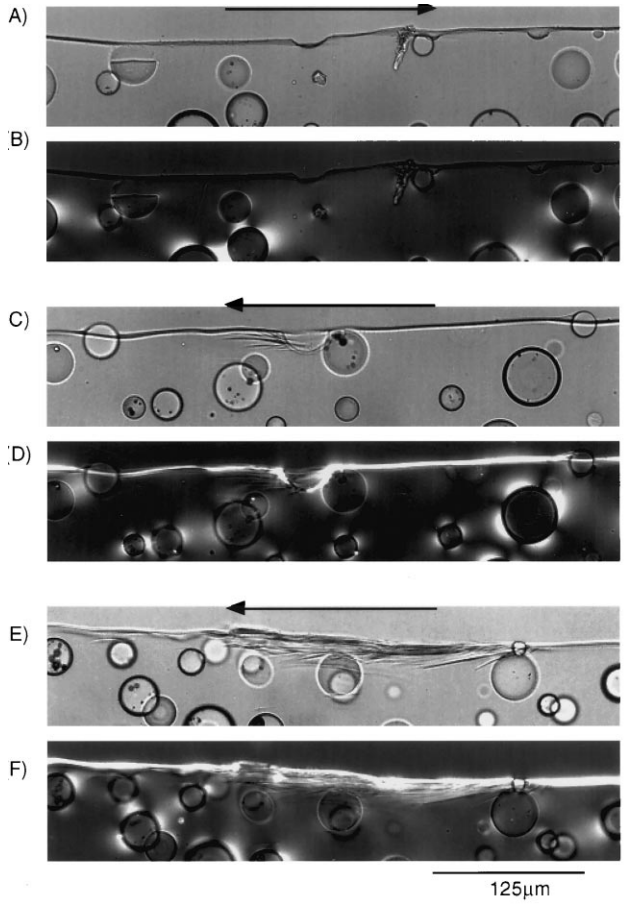

Fig. 3. Transmitted light optical micrographs of thin sections taken near process zone in SEN-3PB specimens: (A) and (B) 10 vol% G/332 (film thickness = 35 μm); (C) and (D) 10 vol% G/664 (film thickness = 43 μm); (E) and (F) 10 vol% G/667 (film thickness = 58 μm), where (A), (C) and (E) were taken without polarizers, and (B), (D) and (F) were taken between crossed polarizers. The arrows indicate the direction of crack propagation.

3.2. Microscopy study I—SEM micrographs

To understand the reason why tougher matrices would achieve a higher toughening effect, the fracture surface (only process zone [29]) of glass bead filled epoxies was examined using scanning electron microscopy (SEM). Fig. 2 shows the fracture surface of two extreme cases, the most brittle matrix system (10 vol% g/332) and the toughest matrix system (10 vol% G/667) among the composites prepared in here. The major deformations that can be found in Fig. 2 are step formation and debonding of glass beads. The step formation [3,4,14,36–42] may be an energy dissipating mechanism, because it generates extra surface area and involves mixed mode fracture. However, it was found that the areal density of steps (length of steps per unit area) did not reflect the increase in toughening effect discussed above [43–46]. The composite with the highest step density was the 10 vol% G/332, followed by 10 vol% G/667. Therefore, energy dissipation through this mechanism was thought to be insignificant. A quantitative analysis on the areal density of steps will be treated in other reports [43–46].

The debonding of glass beads from the matrix [12,47–49] is another deformation mechanism that can be analyzed using SEM. In fact, the debonding zone, a process zone containing debonded glass beads, can be identified using both SEM and OM. The results of debonding zone size measurement are presented in Table 3. They show the increase in size with increasing molecular weight of epoxides. Thus, the increase of toughening effect with the increase of inherent matrix toughness found in Fig. 1 might be explained as follows: the toughening effect increases because of the increase in debonding zone size, so more energy can be dissipated in the debonding of glass beads. In reality, the contribution of the debonding mechanism to toughening may be even more important, because debonding of glass beads can trigger diffuse shear yielding around the craters in the matrix left by debonded particles. Indeed, debonding of glass beads is always accompanied by diffuse shear yielding around the craters as will be found in the following OM micrographs. Thus, the two deformations can be treated as a combined process. A more significant amount of energy can be dissipated by this combined process than by debonding alone.

The plastic zone sizes of unmodified epoxies are given in Table 1. The plastic zone size was calculated from Irwin's equation [20,50] for the plane strain condition:

$$K_{IC} = [3\pi(2r_p)]^{1/2}\sigma_y \quad (5)$$

where σ_y is the yield stress and r_p the plastic zone size. For inorganic particle filled polymers, attempts have already been made to predict the size of process zones using the plastic zone models [51,52]. However, no successful agreement between the predictions from this model and experimental measurements have been reported, and none was found in our experiments either. Koh et al. [51] reported from their experiments on silica filled epoxies that the predicted values from the plastic zone model were not in reasonable agreement with their experimental measurements. They attributed this discrepancy to the inaccurate measurements of yield stress. However, the direct utilization of the models for the study on inorganic particle toughening is not appropriate for two reasons:

1. The models are derived for homogeneous materials. In inorganic particle filled polymers, particle size is usually comparable to or larger than the crack tip radius, and so the stress distribution around the crack tip is significantly perturbed by the existence of inorganic particles.
2. The models consider shear yielding as the only micro-deformation mechanism occurring in the process zone. Clearly, in inorganic particle filled polymers, the effects of other deformation mechanisms, such as microcracking (e.g. debonding of glass beads), should be accounted for.

There can also be interactions among the possible micro-deformation mechanisms.

3.3. Microscopy study II—OM micrographs

The sub-surface damage in inorganic particle filled thermosets has seldom been studied compared to surface damage [53]. This is partially because the macroscopic fracture behavior of these materials is too brittle which might have led previous researchers to neglect sub-surface damage. However, the examination of sub-surface damages turned out to be very useful in the current experiments.

Fig. 3(C)–(F) shows the sub-surface damages in fractured SEN-3PB specimens. Process zones are in the middle of each micrograph. First of all, fine dark lines can be found in these micrographs. Since crazing could occur as the cross-link density decreases, the fine dark lines in these micrographs could be crazes, particularly in the 667 system. Henkee and Kramer [54] proposed a critical cross-link density above which crazing cannot occur. According to them, this value is about 8×10^{25} m^{-3}. The approximate cross-link densities (γ) of the composites prepared here are calculated from M_c as follows:

$$\gamma = \frac{\rho N_A}{M_c} \tag{6}$$

where ρ is the density of epoxies, N_A the Avogadro number. The calculated values are 2.6×10^{27}, 6.1×10^{26}, 3.7×10^{26} and 1.5×10^{26} m^{-3} for 10 vol% G/332, 10 vol% G/661, 10 vol% G/664, and 10 vol% G/667, respectively. These values are well above the critical value proposed by Henkee and Kramer [54]. Therefore, crazing will not likely occur in these composites, although the critical value may not be accurate and appropriate for DGEBA/DDS epoxies. In fact, as the precise critical cross-link density value for our epoxies is not available, it is still not clear whether crazing can occur or not. Moreover, in addition to crazing, microcracking [55] can also occur and leave fine dark lines in Fig. 3.

To determine fine scale deformation mechanisms, TEM microscopy studies on ultra-thin sections of SEN-3PB and DEN-4PB specimens microtomed perpendicular to the crack propagation planes were performed. Also, SEM microscopy studies on cryofractured surfaces perpendicular to the crack propagation planes were performed. Neither microscopy studies show any evidence of crazes or microcracks. Another experiment to identify the nature of the dark lines is by heating thin-sections of DEN-4PB and SEN-3PB specimens. When the temperature reaches about 10°C below T_g of matrix during heating at 0.5°C/min, the fine dark lines completely disappear. If the lines are microcracks, they cannot be healed by thermal energy at this temperature [56], because the interdiffusion rate of macromolecular chains is too low to heal the microcracks, and the restoration of chemical cross-links is nearly impossible [57,58]. From these experiments, it was confirmed that neither crazing nor microcracking occurred during the fracture of the materials studied, and the fine dark lines must therefore be micro-shear bands. The results of this subject are given in detail in other papers [43–46].

Fig. 3 shows noticeable micro-shear bands (fine dark lines) beneath the fracture surface. As inherent matrix toughness increases, the size of the micro-shear band zone is found to increase as well. In 10 vol% G/332, micro-shear bands are invisible, but they are visible in the other three filled systems. In 10 vol% G/661 and 10 vol% G/664, micro-shear bands are usually found around glass beads, but in 10 vol% G/667, they are extensively found in a large region encompassing several glass beads.

Micro-shear banding (inhomogeneous shear yielding) has been studied by many researchers [59–64] and it is generally understood that it occurs due to the strain softening behavior of materials and the existence of initial strain inhomogeneities. Bowden [60] proposed a model to describe the initiation of micro-shear banding

$$\epsilon^C = \epsilon^* \ln\left(\frac{\epsilon^*}{\Delta\epsilon}\right) \tag{7}$$

where ϵ^C is the strain to initiate micro-shear banding, ϵ^* the characteristic strain of materials, and $\Delta\epsilon$ the initial strain inhomogeneity. In glass bead filled epoxies, the existence of glass beads is able to provide large $\Delta\epsilon$ values and the strain softening behavior of epoxies is able to give favorable ϵ^* values. Therefore, it is possible that micro-shear bands initiate from the interface between glass beads and matrix ahead of crack tips, and propagate into the matrix, thus absorbing significant amounts of energy upon subsequent crack growth.

The micrographs taken between crossed polarizers in Fig. 3 show two different kinds of birefringence. One is due to thermal residual misfit stress around glass beads. Since the thermal residual misfit stress is isotropic around a glass bead, cross-extinguished birefringent features are visible around the glass bead [65–70]. The other birefringence is due to diffuse matrix shear yielding. This can be found around the craters, and in all fracture surfaces of 10 vol% G/664 and 10 vol% G/667. This birefringence has more clearly defined boundaries than the birefringence due to thermal residual misfit stress. The crater in Fig. 3(D) clearly shows strong birefringence due to diffuse shear yielding. An interesting thing to note is that the yielded region is wider at the equatorial region than at the pole region of the craters. (The equatorial region refers to the interfacial region between glass beads and the matrix, which is parallel to the direction of the far-field stress. Thus, the uniaxial far-field stress is along the poles.) The debonding of a glass bead creates a cavity in the matrix, and the von Mises stress will be higher at the equatorial region [27,50,71–73]. Therefore it is not surprising that the equatorial region of the craters is more birefringent.

Among the four kinds of epoxy resins, only 664 and 667

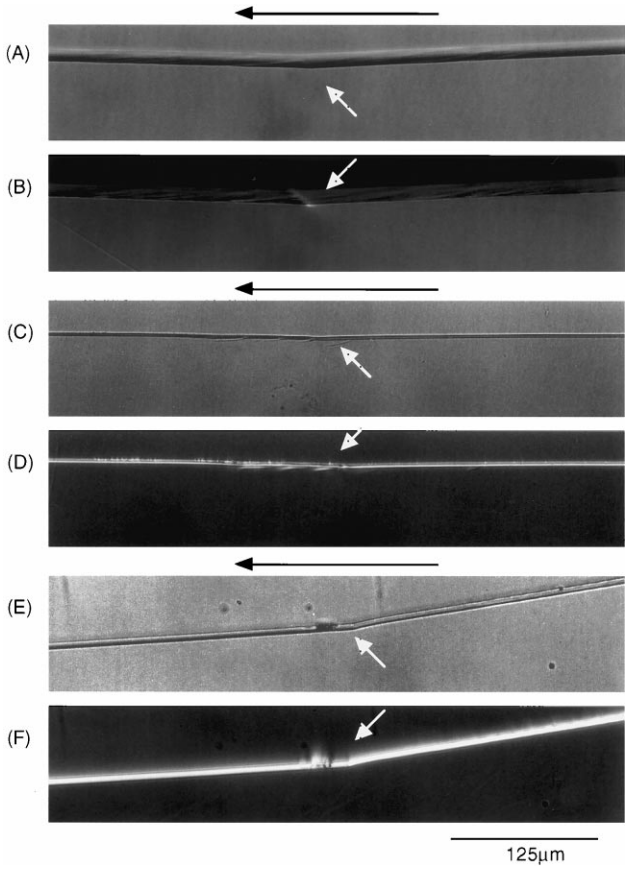

Fig. 4. Transmitted light optical micrographs of thin sections taken near process zone in SEN-3PB specimens: (A) and (B) 332 (film thickness = 64 μm); (C) and (D) 664 (film thickness = 38 μm); (E) and (F) 667 (film thickness = 58 μm), where (A), (C) and (E) were taken without polarizers, and (B), (D) and (F) were taken between crossed polarizers. The arrows indicate the location of process zone.

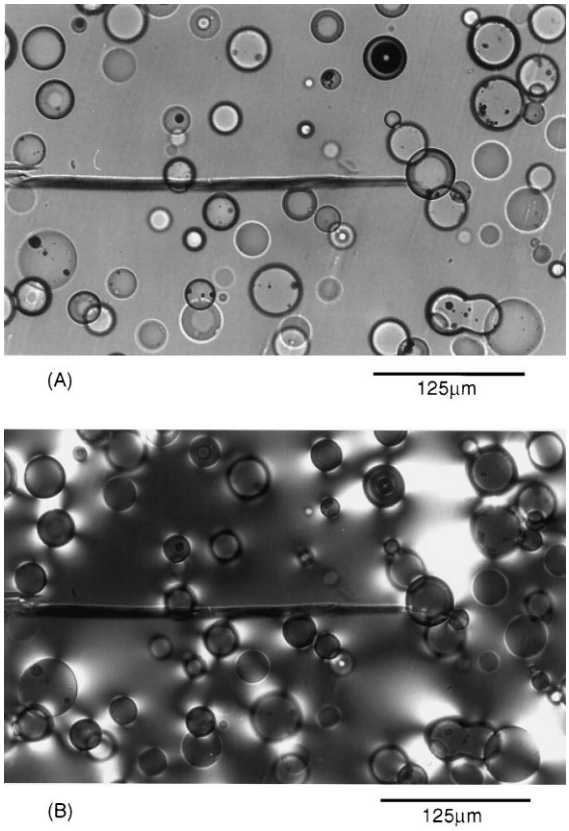

Fig. 5. Transmitted light optical micrographs of a thin section taken near the tip of a sub-critically loaded crack in a DEN-4PB specimen of 10 vol% G/332 (film thickness = 43 μm): (A) without polarizers; (B) the same region as that in (A), but between crossed polarizers.

systems exhibit significant diffuse matrix shear yielding in their fracture surface regions, which is not confined to the crater region, and can be found even in fast-fracture regions (Fig. 3). Therefore, this shear yielding appears to be dependent not on the existence of glass beads but only on inherent matrix properties. This conjecture is verified by examining the sub-surface damage in fractured specimens of unmodified epoxies (Fig. 4). The same birefringence as those in Fig. 3 can be found in Fig. 4. The 664 and 667 resins exhibit a thin shear yielded region along the entire fracture surface. Even in the brittle 332 resin, birefringence can be found in a very small area in the middle of Fig. 4(B). This area is the process zone. While birefringent regions are found in 332 resin, no such regions can be found in 10 vol% G/332 in Fig. 3. However, in glass bead filled epoxies, the birefringence due to thermal residual misfit and the existence of glass beads can obscure the very small birefringent region. We expect that the same matrix shear yielding can occur even in glass bead filled 332 epoxies.

For unmodified epoxies, Dougdale's plastic zone model or Irwin's model (Eq. (5)) can give the estimated size of the plastic zones [20,50]. The calculated values from Irwin's model in Table 1 are significantly larger than the sizes of birefringent regions in Fig. 4. They are about 8 and 16 μm for the 664 and 667 resins, respectively. Dougdale's plastic zone model predicts a plastic zone size 2.5 times larger than Irwin's, which still disagrees with the sizes of birefringent regions in Fig. 4. Therefore, the size of the birefringent region may not reflect the size of the plastic zone or those predicted by the models.

Figs. 5–7 show the OM micrographs of sub-critically loaded cracks. The evidence of birefringence due to thermal residual misfit, i.e. the characteristic cross-extinguished birefringent feature [66–70], can be observed in all micrographs taken using two crossed polarizers. It can also be found in these micrographs that the birefringence around most glass beads is not distorted by the crack tip stress field. Accordingly, it can be surmised that the crack tip stress field can interact with the misfit stress in only small regions where the glass beads come into contact with the fracture surface or crack tip.

In Fig. 5, the crack path in 10 vol% G/332 ends up with a sharp crack tip without having any noticeable damage. On the other hand, all the other three systems show distinct micro-shear bands at crack tips and ahead of crack tips (Figs. 6 and 7). More interestingly, the size of the

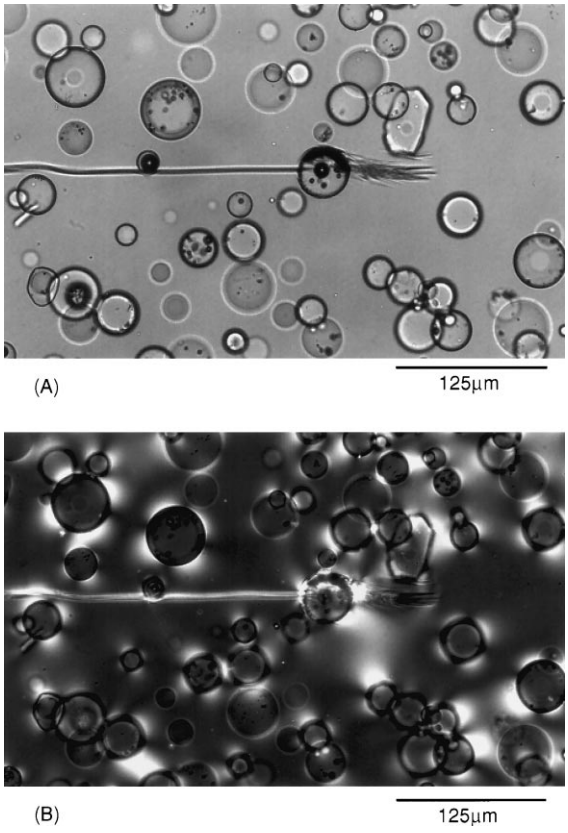

Fig. 6. Transmitted light optical micrographs of a thin section taken near the tip of a sub-critically loaded crack in a DEN-4PB specimen of 10 vol% G/664 (film thickness = 50 μm): (A) without polarizers; (B) the same region as that in (A), but between crossed polarizers.

micro-shear band zone increases with increasing molecular weight of epoxides. Consequently, the energy absorbed by micro-shear banding will increase as well with the increase of the molecular weight. Therefore, micro-shear banding can explain why the toughening effect of glass bead incorporation into epoxies increases with the molecular weight of epoxides. As the molecular weight increases, i.e. as the cross-link density decreases, the intrinsic ductility of epoxy matrix may increase, resulting in more extensive micro-shear banding.

Although most micro-shear bands are developed from the glass beads at the crack tip, isolated micro-shear bands from the crack tip can also be found in Figs. 6 and 7. These seem to be initiated from the pole regions of glass beads and propagate in the direction approximately parallel to the crack path. Since glass beads have modulus one order of magnitude higher than the epoxy matrix, stress will be concentrated around glass beads in composites, resulting in the initiation of micro-shear banding. In Fig. 7, there is a micro-shear band around a glass bead at the crack tip region, which is not visible as a sharp dark line in (A), but birefringent in (B). It is indicated by an arrow in Fig. 7. This is an interesting additional piece of evidence for the identity of micro-shear bands.

Since the 10 vol% G/332 system does not show any micro-shear bands in its process zone (Fig. 5), it follows that the micro-shear banding mechanism cannot be the major toughening mechanism for brittle matrix systems, such as those based on the 332 resin. Accordingly, the toughness increase found in 332 systems is much smaller than that found in other tougher matrix systems (Fig. 1). Micro-shear banding and debonding/diffuse matrix shear yielding, if any, are likely to be the major contributions to toughening by the addition of glass beads into epoxies.

4. Conclusions

In summary, several glass bead filled epoxies having different inherent matrix toughness values were prepared and their fracture behaviors were examined. The inherent matrix toughness was varied by changing the molecular weight of epoxides. It was demonstrated that the fracture toughness of glass bead filled epoxies increased as the inherent matrix toughness increased. The toughening effect of glass bead incorporation represented by K_{IC}(modified)/K_{IC}(unmodified) or G_{IC}(modified)/G_{IC}(unmodified) was observed to increase with increasing inherent matrix toughness. Therefore, it could be stated that the use of glass beads as tougheners was more effective in tougher epoxy matrices.

From various microscopy studies, several micro-deformation mechanisms were observed to occur during the fracture of glass bead filled epoxies, i.e. step formation, debonding of glass beads, diffuse matrix shear yielding, and micro-shear banding. It was noticed that the areal density of steps was not linearly proportional to the fracture toughness of composites. In all the unmodified and glass bead filled 664 and 667 systems, distinct diffuse shear yielded regions were found along the fracture surface. Even in the most brittle epoxy resin, 332, a small but distinct shear yielded region was found. Besides the diffuse shear yielded regions found along fracture surfaces regardless of the existence of glass beads, surface crater regions show matrix shear yielding around them. As inherent matrix toughness increases, micro-shear banding, debonding of glass beads, and diffuse matrix shear yielding were found to be more prevalent deformation mechanisms. Therefore, the increase of toughening effect of glass beads with the increase of inherent matrix toughness could be attributed to the accompanying increase in micro-shear banding and debonding/diffuse shear yielding. The results of the current experiments show that the localized shear yielding of the matrix was most likely to be the major energy absorption mechanism for both unmodified and glass bead filled epoxies.

Acknowledgements

This work was supported by the Specialized Materials Science Research Center of National Institute of Health

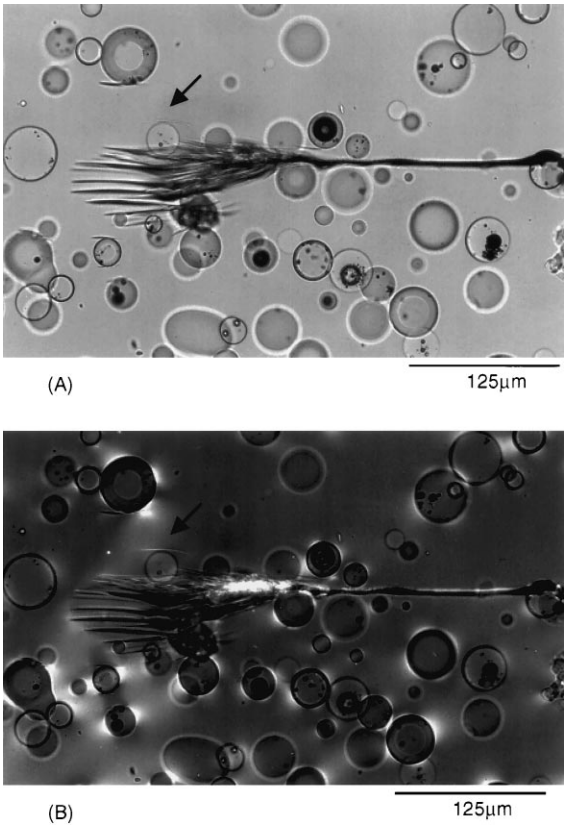

Fig. 7. Transmitted light optical micrographs of a thin section taken near the tip of a sub-critically loaded crack in a DEN-4PB specimen of 10 vol% G/667 (film thickness = 30 μm): (A) without polarizers; (B) the same region as that in (A), but between crossed polarizers.

(NIH), under a contract No. DEO 9296-09. The authors would like to thank Dr Hajime Kishi, Dr Jack Huang, Dr Yu Shen and Ms Jacqueline M. Denoyer for their help.

References

[1] Pearson RA, Yee AF. J Mater Sci 1989;24:2571.
[2] LeMay JD, Kelley FN. Adv Polym Sci 1986;78:115.
[3] Spanoudakis J, Young RJ. J Mater Sci 1984;19:473.
[4] Spanoudakis J, Young RJ. J Mater Sci 1984;19:487.
[5] Nakamura Y, Yamaguchi M, Okubo M, Matsumoto T. Polymer 1991;32:2221.
[6] Nakamura Y, Yamaguchi M, Okubo M, Matsumoto T. Polymer 1991;32:2976.
[7] Nakamura Y, Yamaguchi M, Okubo M, Matsumoto T. Polymer 1992;33:3415.
[8] Nakamura Y, Yamaguchi M, Okubo M, Matsumoto T. J Appl Polym Sci 1992;44:151.
[9] Nakamura Y, Yamaguchi M, Okubo M, Matsumoto T. J Appl Polym Sci 1992;45:1281.
[10] Nakamura Y, Yamaguchi M, Okubo M. Polym Engng Sci 1993;33:279.
[11] Kinloch AJ, Maxwell DL, Young RJ. J Mater Sci 1985;20:4169.
[12] Rothon R. Particulate-filled polymer composites. New York: Longman, 1995.
[13] Lavengood RE, Nicolais L, Markis M. J Appl Polym Sci 1973;17:1173.
[14] Lange FF. Philos Mag 1970;22:983.
[15] Evans AG. Philos Mag 1972;26:1327.
[16] Green DJ, Nicholson PS, Embury JD. J Mater Sci 1977;12:987.
[17] Green DJ, Nicholson PS, Embury JD. J Mater Sci 1979;14:1413.
[18] Green DJ, Nicholson PS, Embury JD. J Mater Sci 1979;14:1657.
[19] Rice JR, Ben-Zion Y, Kim K. J Mech Phys Solids 1994;42:813.
[20] Kinloch AJ, Young RJ. Fracture behavior of polymers. Amsterdam: Elsevier, 1985.
[21] Evans AG. Private discussion, 1998.
[22] Moloney AC, Kausch HH, Stieger HR. J Mater Sci 1983;18:208.
[23] Sahu S, Broutman LJ. Polym Engng Sci 1972;12:91.
[24] Broutman LJ, Shau S. Mater Sci Engng 1971;8:98.
[25] Ferry JD. Viscoelastic properties of polymers. 3 ed.. New York: Wiley, 1980.
[26] Brown WF, Srawley JE. ASTM STP 1965;381:13.
[27] Hertzberg RW. Deformation and fracture mechanics of engineering materials. New York: Wiley, 1989.
[28] Sue HJ, Yee AF. J Mater Sci 1993;28:2975.
[29] Pearson RA, Yee AF. J Mater Sci 1986;21:2475.
[30] Holik AS, Kambour RP, Hobbs SY, Fink DG. Microstr Sci 1979;7:367.
[31] Sawyer LC, Grubb DT. Polymer microscopy. New York: Chapman and Hall, 1987.
[32] Bos HL, Nusselder JJ. Polymer 1994;35:2793.
[33] Glad MD, Kramer EJ. J Mater Sci 1991;26:2273.
[34] Nielsen LE. J Macromol Sci 1969;C-3:69.
[35] Bellenger V, Verdu J. J Polym Sci B 1987;25:1219.
[36] Atsuta M, Turner DT. J Mater Sci 1982;1:167.
[37] Kinloch AJ, Gilbert D, Shaw SJ. Polym Commun 1985;26:290.
[38] Purslow D. Composites 1986;17:289.
[39] Hull D. Int J Fracture 1993;62:119.
[40] Hull D. Int J Fracture 1995;70:59.
[41] Hull D. J Mater Sci 1996;31:1829.
[42] Hull D. J Mater Sci 1996;31:4483.
[43] Lee J, Yee AF. In preparation.
[44] Lee J. PhD thesis, The University of Michigan, 1998.
[45] Lee J, Yee AF. Polym Prep, Am Chem Soc Div Polym Chem 1997;38:369.
[46] Lee J, Yee AF. Polym Prepr, Am Chem Soc Div Polym Mater 1998;79:200.
[47] Pukanszky B, Van Es MJ, Maurer FH, Voros G. J Mater Sci 1994;29:2350.
[48] Zhong XA, Knauss WG. J Engng Mater Technol 1997;119:199.
[49] Williams JG. Fracture mechanics of polymers. 1 ed.. Chichester, UK: Ellis Horwood, 1984.
[50] Young RJ, Beaumont PWR. J Mater Sci 1977;12:684.
[51] Koh S, Kim J, Mai Y. Polymer 1993;34:3446.
[52] Moloney AC, Kausch HH, Kaiser T, Beer HR. J Mater Sci 1987;22:381.
[53] Vekinis G, Beaumont PWR, Pritchard G, Wainwright P. J Mater Sci 1991;26:4527.
[54] Henkee CS, Kramer EJ. J Polym Sci, Polym Phys Ed 1984;22:721.
[55] Azimi HR, Pearson RA, Hertzberg RW. Polym Engng Sci 1996;36:2352.
[56] Kausch HH. Polymer fracture. Berlin: Springer, 1987.
[57] Kausch HH, Petrovska D, Landel RF, Monnerie L. Polym Engng Sci 1987;27:149.
[58] Davies P, Cantwell W, Kausch HH. J Mater Sci 1989;8:1247.
[59] Argon AS, Andrews RD, Godrick JA, Whitney W. J Appl Phys 1968;39:1899.
[60] Bowden PB. Philos Mag 1970;25:455.
[61] Bowden PB, Raha S. Philos Mag 1970;25:463.
[62] Kramer EJ. J Polym Sci, Polym Phys Ed 1975;13:509.
[63] Wu JBC, Li JBC. J Mater Sci 1976;11:434.
[64] Li JBC, Wu JBC. J Mater Sci 1976;11:445.

[65] Clyne TW, Withers PJ. An introduction to metal matrix composites. New York: Cambridge University, 1993.
[66] Chow TS, Wilson JC. J Polym Sci. B 1978;16:967.
[67] Evans AG. J Mater Sci 1974;9:1145.
[68] Wang H, Li S, Zhou H, Yu T, Jin X. Polym Engng Sci 1992;32:678.
[69] Wang H, Li S, Yu T. Polym Engng Sci 1993;33:474.
[70] Fan CF, Hsu SL. J Polym Sci B 1992;30:603.
[71] Goodier JN. J Appl Mech 1933;55(A39):39.
[72] Broutman LJ, Agarwal BD. Polym Engng Sci 1974;14:581.
[73] Ricco T, Pavan A, Danusso F. Polym Engng Sci 1978;18:774.